Dynamic Multi-Objective Optimization of Integrated Energy Systems in Steel Enterprises via Conditional Variational Autoencoder

Min Chen
National Frontiers Science Center for
Industrial Intelligence and Systems Optimization
Northeastern University, Shenyang 110819, China
chenmin060621@gmail.com

Shengxiang Yang
School of Computer Science and Informatics
De Montfort University, Leicester LE1 9BH, UK
syang@dmu.ac.uk

Yanyan Zhang
National Frontiers Science Center for
Industrial Intelligence and Systems Optimization
Northeastern University, Shenyang 110819, China
zhangyanyan@ise.neu.edu.cn

Shengnan Zhao
National Frontiers Science Center for
Industrial Intelligence and Systems Optimization
Northeastern University, Shenyang 110819, China
zhaoshengnan@mail.neu.edu.cn

***Abstract*—To overcome the limitations of conventional evolutionary algorithms in dynamic integrated energy systems for steel enterprises, this paper proposes a Conditional Variational Autoencoder (CVAE) guided multi-objective optimization framework. The method minimizes operational costs and external energy reliance by using online-trained CVAE to map dynamic environmental states (e.g., energy loads, price signals) to optimal solution distributions. Upon detecting changes, the model rapidly generates a state-conditioned initial population, providing a warm start for the evolutionary search. Experiments verify that this framework significantly accelerates convergence and improves solution stability and economic performance in dynamic environments.**

***Index Terms*—Dynamic integrated energy scheduling, steel enterprise energy systems, conditional variational autoencoder, dynamic multi-objective optimization.**

I. INTRODUCTION

The steel industry is one of the largest energy consumers and carbon emitters worldwide, particularly in China, where it accounts for a substantial share of total industrial energy consumption [1]. Modern steel enterprises are typically equipped with integrated energy systems that coordinate multiple energy carriers, including electricity, gas, steam, and heat, through tightly coupled conversion and storage devices [2].

Efficient scheduling of such integrated energy systems is crucial for reducing operational costs, improving energy self-sufficiency, and mitigating environmental impacts, which are often conflicting objectives in practice [3]. Moreover, the scheduling process is inherently dynamic due to time-varying load demands, fluctuating energy prices, and the intermittency of renewable energy generation, naturally formulating the problem as a dynamic multi-objective optimization task that challenges conventional static methods.

In recent years, dynamic multi-objective evolutionary algorithms (DMOEAs) have been widely studied for handling dynamic optimization problems [4], [5]. However, most existing approaches are designed for generic benchmark problems and do not explicitly account for the strong multi-energy coupling, complex operational constraints, and interaction mechanisms present in steel enterprise integrated energy systems.

To address these challenges, this study presents CVAE-MOEA/D, a CVAE-assisted dynamic multi-objective optimization framework that integrates a conditional variational autoencoder into MOEA/D-ϵ [6], [7] to improve adaptability to dynamic environments.

Specifically, CVAE [8] is used to learn condition-dependent distributions of high-quality scheduling solutions under varying states of the system. By capturing the relationship between environmental conditions and promising solution regions, CVAE enables adaptive solution generation in response to time-varying load demands, energy prices, and renewable energy availability, thereby improving the efficiency and robustness of evolutionary search. The main contributions of this work are summarized as follows:

- A dynamic bi-objective optimization model is formulated for integrated energy systems in steel enterprises under time-varying operating conditions.
- A CVAE-assisted evolutionary optimization framework is proposed to enhance adaptability in dynamic environments.
- Comparative simulations on a realistic steel enterprise energy scheduling case demonstrate improved economic efficiency and energy self-sufficiency.

II. Dynamic Integrated Energy Scheduling Model

A. System Description

Fig. 1 illustrates the studied integrated energy system, which couples gas generators, boilers, steam turbines, electrical storage, and Wind Turbine / Photovoltaic (WT/PV) units via gas, electricity, heat, and steam carriers. All notations, variables, and parameters used in the model are summarized in Table I.

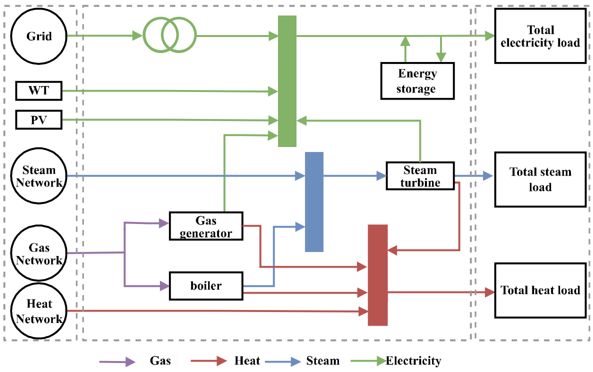

Fig. 1: Schematic of the integrated energy system.

B. Objective Functions

The problem is formulated as:

$$\min \mathbf{F}(x,t) = (f_1, f_2) \tag{1}$$

1) Operating Cost: The objective is to minimize the total operating cost of the integrated energy system over the scheduling horizon, defined as follows:

$$f_1 = \sum_{t=1}^{T} \Big(C_{\text{gas}}(t) + C_{\text{heat}}(t) + C_{\text{grid}}(t) + C_{\text{steam}}(t) - R_{\text{stor}}(t) \Big) \tag{2}$$

where the cost components for gas, heat, grid electricity, and steam are calculated by multiplying their respective power consumption by the unit prices:

$$\begin{aligned} C_{\text{gas}}(t) &= P_{\text{gas}}(t) c_{\text{gas}}(t) \qquad C_{\text{heat}}(t) = P_{\text{heat}}(t) c_{\text{heat}}(t) \\ C_{\text{grid}}(t) &= P_{\text{grid}}(t) c_{\text{grid}}(t) \quad C_{\text{steam}}(t) = P_{\text{steam}}(t) c_{\text{steam}}(t) \end{aligned} \tag{3}$$

and the economic benefit of the energy storage system is expressed as follows:

$$R_{\text{stor}}(t) = P_{\text{char}}(t)\lambda_L(t) + P_{\text{dischar}}(t)\lambda_H(t) \tag{4}$$

The gas consumption at time t is calculated as

$$P_{\text{gas}}(t) = \left(\left(P_{\text{gen,e}}(t)\Delta t\right)/\eta_{\text{gen}} + \left(P_{\text{boiler,s}}(t)\Delta t\right)/\eta_{\text{boiler}} \right) / \text{Cal}_{\text{gas}} \tag{5}$$

2) External Energy Supply Rate: The dependence of the system on external energy sources is reduced by maximizing the self-sufficiency of electricity, heat, and steam.

$$\min f_2 = \eta_{\text{ext}} = 1 - 1/3\left(e_{\text{rate}} + h_{\text{rate}} + s_{\text{rate}}\right) \tag{6}$$

where the rates of self-sufficiency for electricity, heat and steam at time t are defined as follows:

$$e_{\text{rate}}(t) = \left(P_{\text{gen,e}}(t) + P_{\text{turbine,e}}(t) + P_{\text{WT}}(t) + P_{\text{PV}}(t)\right)/e_{\text{load}}(t) \tag{7}$$

$$h_{\text{rate}}(t) = \left(P_{\text{gen,h}}(t) + P_{\text{turbine,h}}(t) + P_{\text{boiler,h}}(t)\right)/h_{\text{load}}(t) \tag{8}$$

$$s_{\text{rate}}(t) = P_{\text{boiler,s}}(t)/s_{\text{load}}(t) \tag{9}$$

The coupling relationships among electricity, heat, and steam are given by

$$P_{\text{gen,h}}(t) = P_{\text{gen,e}}(t)/\eta_{\text{gen}} - P_{\text{gen,e}}(t) \tag{10}$$

$$P_{\text{turbine,h}}(t) = P_{\text{turbine,e}}(t)/\eta_{\text{turbine}} - P_{\text{turbine,e}}(t) \tag{11}$$

$$P_{\text{boiler,h}}(t) = P_{\text{boiler,s}}(t)/\eta_{\text{boiler}} \cdot \eta_{\text{boiler,h}} \tag{12}$$

C. Operational Constraints

1) Energy Balance Constraints: The energy supply and demand (electricity, steam, heat) must be balanced in each period t.

- Electricity Balance

$$\begin{aligned} &P_{\text{grid}}(t) + P_{\text{PV}}(t) + P_{\text{WT}}(t) + P_{\text{gen,e}}(t) \\ &+ P_{\text{turbine,e}}(t) + P_{\text{dischar}}(t) = e_{\text{load}}(t) + P_{\text{char}}(t) \end{aligned} \tag{13}$$

- Steam Balance

$$P_{\text{steam}}(t) + P_{\text{boiler,s}}(t) - P_{\text{turbine,s}}(t) = s_{\text{load}}(t) \tag{14}$$

The steam consumption of the turbine is related to its electricity output by

$$P_{\text{turbine,s}}(t) = P_{\text{turbine,e}}(t)/\eta_{\text{turbine}} \tag{15}$$

- Heat Balance

$$P_{\text{gen,h}}(t) + P_{\text{boiler,h}}(t) + P_{\text{turbine,h}}(t) + P_{\text{heat}}(t) = h_{\text{load}}(t) \tag{16}$$

2) Energy Storage Operation Constraints:

- Charging and Discharging Power Limits

$$P_{\text{char}}(t)\, P_{\text{dischar}}(t) = 0 \tag{17}$$

$$0 \le P_{\text{char}}(t) \le P_{\text{char}}^{\max} \tag{18a}$$

$$P_{\text{char}}(t) \le (\text{SOC}_{\max} - \text{SOC}(t))C_{\text{EES}}/(\eta_{\text{char}}\Delta t) \tag{18b}$$

$$0 \le P_{\text{dischar}}(t) \le P_{\text{dischar}}^{\max} \tag{19a}$$

$$P_{\text{dischar}}(t) \le (\text{SOC}(t) - \text{SOC}_{\min})C_{\text{EES}}\eta_{\text{dischar}}/\Delta t \tag{19b}$$

- State of Charge (SOC) Constraints

$$\text{SOC}_{\min} \le \text{SOC}(t) \le \text{SOC}_{\max} \tag{20}$$

$$\text{SOC}(1) = \text{SOC}(T) \tag{21}$$

$$|\text{SOC}(t) - \text{SOC}(t-1)| \le \Delta_{\text{SOC}} \tag{22}$$

$$\begin{aligned} \text{SOC}(t+1) = {} & \text{SOC}(t) + \eta_{\text{char}} P_{\text{char}}(t)\Delta t / C_{\text{EES}} \\ & - P_{\text{dischar}}(t)\Delta t/(\eta_{\text{dischar}} C_{\text{EES}}) \end{aligned} \tag{23}$$

TABLE I: Notation Used in the Integrated Energy Scheduling Model

Symbol	Description	Unit
Indexes		
t	Index of scheduling time periods, $t = 1, 2, \ldots, T$	–
Parameters		
$c_{\text{grid}}(t)$, $c_{\text{gas}}(t)$, $c_{\text{heat}}(t)$, $c_{\text{steam}}(t)$	Time-varying prices of electricity, gas, heat, and steam at time t	–
$\lambda_L(t)$, $\lambda_H(t)$	Electricity prices for charging and discharging of the energy storage system	CNY/MWh
η_{gen}, η_{boiler}, η_{turbine}	Energy conversion efficiencies of gas generators, boilers, and steam turbines	–
$\eta_{\text{boiler,h}}$	Heat recovery efficiency of gas boilers	–
η_{char}, η_{dischar}	Charging and discharging efficiencies of the energy storage system	–
Cal_{gas}	Lower calorific value of natural gas	MJ/m^3
C_{EES}	Rated energy capacity of the energy storage system	MWh
$\text{SOC}_{\min}$, $\text{SOC}_{\max}$	Lower and upper bounds of the state of charge (SOC)	–
$P_{\text{char}}^{\max}$, $P_{\text{dischar}}^{\max}$	Maximum charging and discharging power of the energy storage system	MW
Δt, Δ_{SOC}	Length of scheduling interval and maximum allowable SOC variation (20%)	–
$e_{\text{load}}(t)$, $h_{\text{load}}(t)$, $s_{\text{load}}(t)$	Electricity, heat, and steam demand at time t	MW
Decision Variables		
$P_{\text{gen,e}}(t)$, $P_{\text{turbine,e}}(t)$	Electricity output power of gas generators and steam turbines at time t	MW
$P_{\text{boiler,s}}(t)$	Steam output power of gas boilers at time t	MW
$P_{\text{steam}}(t)$, $P_{\text{heat}}(t)$	Steam and heat supplied by the corresponding energy networks at time t	MW
$P_{\text{grid}}(t)$	Electricity purchased from the external power grid at time t	MW
$P_{\text{char}}(t)$, $P_{\text{dischar}}(t)$	Charging and discharging power of the energy storage system at time t	MW

3) Operational Limits: All decision variables are subject to operational limits, including capacity bounds and ramping constraints, to reflect physical capacities, technical restrictions, and intertemporal operational continuity of energy system components.

III. Methodology

A. Overall Framework

The overall framework of CVAE-MOEA/D is illustrated in Fig. 2, which outlines the interaction between conditional population generation and evolutionary optimization across successive time steps. To facilitate reproducibility and implementation, the main procedure of the proposed method is summarized in Algorithm 1.

B. Conditional Representation and Change Detection

To explicitly model time-varying conditions (demands, prices, and system states), the environmental state at time t is defined as:

$$Env_t = \left[\mathbf{d}_t, \mathbf{p}_t, \mathbf{e}_t^d, \mathbf{e}_t^{ge}\right] \tag{24}$$

where $\mathbf{d}_t$ denotes the energy load information, $\mathbf{p}_t$ represents the energy price signals, $\mathbf{e}_t^d$ indicates the dynamic energy demands of each device, and $\mathbf{e}_t^{ge}$ represents the energy generated by wind turbine and photovoltaic at time t.

A condition vector c_t is constructed by aggregating the environmental state Env_t, transforming the dynamic optimization process into a sequence of condition-dependent tasks. This formulation provides a unified interface for the generative model to learn and exploit solution distributions under varying system states. To ensure training stability and convergence, all components of c_t are normalized to a consistent scale, thereby eliminating disparities among heterogeneous variables.

Furthermore, a change detection mechanism is triggered if the relative variation of any critical component in Env_t

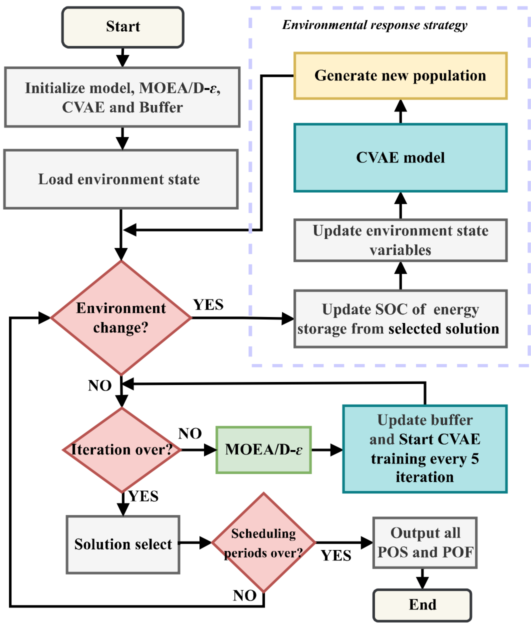

Fig. 2: Framework of the CVAE-MOEA/D.

(i.e., energy prices, renewable generation, or load) exceeds a sensitivity threshold δ. An environmental change is detected at time t if:

$$\max_i \left(\|Env_t^{(i)} - Env_{t-1}^{(i)}\| / \|Env_{t-1}^{(i)}\| \right) > \delta \tag{25}$$

For the specific steel IES case study, the threshold is set as $\delta = 0.05$. This value effectively balances computational efficiency with the sensitivity required to capture significant environmental shifts that alter the Pareto optimal front, ensur-

Algorithm 1: CVAE-MOEA/D

Input: Total scheduling periods T, population size N, replay buffer $\mathcal{B}$, condition vector $\{Env_t\}_{t=1}^{T}$, CVAE training epochs E_{cvae}

Output: Pareto optimal sets $\{POS_t\}_{t=1}^{T}$ and Pareto optimal fronts $\{POF_t\}_{t=1}^{T}$

Initialize population P with N solutions
Initialize CVAE parameters θ
for $t \leftarrow 1$ **to** T **do**
  Get condition vector $c_t \leftarrow \text{Cond}(Env_t)$
  Evaluate population P under Env_t
  if $\text{DetectChange}(Env_t, Env_{t-1}, \delta) = \text{false}$ **then**
    `// environment unchanged`
    Rank solutions in P by $\text{TOPSIS}(\cdot)$ and select top $0.2N$ solutions S_{20}
    Select samples $S \leftarrow \{x \in P \mid x \text{ is feasible}\} \cup S_{20}$
    Store (x, c_t) for all $x \in S$ into replay buffer $\mathcal{B}$; Train CVAE on mini-batches sampled from $\mathcal{B}$ for E_{cvae} epochs
  else `// environment changed`
    Select a solution $x_t^\star \leftarrow \text{TOPSIS}(POF_t)$
    Update $c_{t+1} \leftarrow \text{Cond}(Env_{t+1})$
    Generate a new population $P \sim p_\theta(x \mid c_{t+1})$ using CVAE
  Apply MOEA/D-ϵ to evolve population P under static environment Env_t
return $\{POS_t\}_{t=1}^{T}, \{POF_t\}_{t=1}^{T}$

ing the CVAE-based re-initialization is activated only when necessary.

C. CVAE-Guided Dynamic Population Generation

Based on the conditional formulation in Section III-B, CVAE is employed to guide population generation under time-varying environments. Let c_t denote the condition vector at time step t. CVAE models a condition-dependent generative distribution by decoding a latent variable z together with c_t:

$$x \sim p_\theta(x \mid z, c_t), \quad z \sim \mathcal{N}(\mathbf{0}, \mathbf{I}) \tag{26}$$

where θ denotes the decoder parameters and x is a candidate solution in the decision space.

During the evolutionary process, feasible solutions and nondominated solutions obtained at different time steps are collected to form a training set $\mathcal{D} = (x, c_t)$. The CVAE is updated online to capture the mapping from system conditions to promising solution regions. When an environmental change is detected at time t, the trained decoder is used to generate a batch of candidate solutions:

$$P_t^{\text{new}} = \{x_i^{\text{new}} \mid x_i^{\text{new}} = g_\theta(z_i, c_t),\ i = 1, \ldots, N\}. \tag{27}$$

where $g_\theta(\cdot)$ denotes the decoding function and N is the number of generated solutions. The generated set P_t^{new} is then used to initialize or augment the evolutionary population, providing a warm start under the updated conditions. The evolutionary multi-objective optimizer further refines the population through variation and selection, and the resulting nondominated solutions are fed back to update $\mathcal{D}$ and the CVAE, forming a closed-loop learning and optimization process:

$$\mathcal{D} \leftarrow \mathcal{D} \cup (x, c_t) \mid x \in POF_t \tag{28}$$

To prevent the training buffer from growing unbounded and to avoid the adverse impact of outdated samples, the buffer dataset $\mathcal{D}$ is periodically maintained by removing obsolete or low-quality solutions, thereby preserving a compact and representative set of condition-solution pairs for online CVAE training.

D. CVAE Training

CVAE is composed of an encoder $q_\phi(z \mid x, c_t)$ and a decoder $p_\theta(x \mid z, c_t)$, where ϕ and θ denote the parameters of encoder and decoder, respectively. The encoder learns a latent representation of decision variables conditioned on the dynamic environmental state, while the decoder models the conditional distribution of feasible solutions under the same condition.

Given a training sample $(x, c_t) \in \mathcal{D}$, the encoder outputs the parameters of a Gaussian posterior distribution,

$$q_\phi(z \mid x, c_t) = \mathcal{N}\big(\boldsymbol{\mu}_\phi(x, c_t), \boldsymbol{\Sigma}_\phi(x, c_t)\big) \tag{29}$$

where $\boldsymbol{\mu}_\phi(\cdot)$ and $\boldsymbol{\Sigma}_\phi(\cdot)$ represent the mean vector and diagonal covariance matrix produced by the encoder. The latent variable is sampled using the reparameterization trick, as follows:

$$z = \boldsymbol{\mu}_\phi + \boldsymbol{\Sigma}_\phi^{1/2}\boldsymbol{\epsilon}, \quad \boldsymbol{\epsilon} \sim \mathcal{N}(\mathbf{0}, \mathbf{I}) \tag{30}$$

which enables efficient gradient-based optimization.

CVAE is trained by maximizing the conditional evidence lower bound (ELBO), defined as:

$$\begin{aligned} \mathcal{L}(\theta, \phi) = \ & \mathbb{E}_{q_\phi(z \mid x, c_t)}[\log p_\theta(x \mid z, c_t)] \\ & - \text{KL}(q_\phi(z \mid x, c_t) \parallel p(z)) \end{aligned} \tag{31}$$

where $p(z) = \mathcal{N}(\mathbf{0}, \mathbf{I})$ denotes the prior distribution over latent variables. The first term encourages an accurate reconstruction of the decision variables under the given condition, while the second term regularizes the latent space to ensure smoothness and generalization.

During the dynamic optimization process, CVAE is trained online using mini-batches sampled from the dataset $\mathcal{D}$, which is continuously updated with high-quality solutions obtained from the evolutionary search. This online training strategy enables CVAE to adapt its conditional distribution to changing system conditions.

E. Evolutionary Search and Update

After CVAE-guided population generation, an evolutionary multi-objective optimizer is employed to further refine the candidate solutions under the current environment. Let P_t denote the population at time step t, which consists of both previously evolved solutions and CVAE-generated candidates. Standard evolutionary operators are applied to explore the decision space and improve solution quality.

At each generation, variation operators such as crossover and mutation are used to produce offspring solutions. The fitness of each solution is evaluated according to the objective vector $f(x,t)$, and a decomposition-based selection mechanism is adopted to guide the search toward the Pareto front. Specifically, for a given weight vector $\boldsymbol{\lambda}$, the aggregation value of a solution x is computed as

$$g(x \mid \boldsymbol{\lambda}, z_t^*) = \max_{m=1,\ldots,M} \lambda_m |f_m(x,t) - z_m^*(t)| \tag{32}$$

where z_t^* denotes the ideal point at time step t.

Based on the aggregation values, inferior solutions are replaced by better-performing offspring within each subproblem neighborhood, resulting in an updated population P_t. The nondominated solutions extracted from P_t form an approximation of POF_t under the current environment. These solutions are subsequently used both for performance evaluation and for updating the training data of CVAE, enabling continuous knowledge accumulation across time steps.

IV. Experimental Study

A. Experimental Setting

1) Case Parameters: The system is scheduled over a 24-hour horizon ($T = 24$) with time-varying load, WT/PV generation, and TOU pricing. Device parameters, including battery capacities, power bounds, and efficiencies, are predefined constants.

2) Comparison Algorithms: To evaluate the effectiveness of CVAE-MOEA/D, several representative algorithms are selected for comparison, including DMOEA/D [6], Dynamic NSGA-II (DNSGA-II) [9] with reinitialization (A) and random injection variants (B), and the population prediction strategy (PPS) [10] implemented with NSGA-II and MOEA/D as PPS-NSGA-II and PPS-MOEA/D. All compared algorithms are implemented according to their original descriptions and evaluated under identical experimental settings and dynamic scenarios.

3) Algorithm Settings and Performance Metrics: Algorithm settings include SBX, polynomial mutation, and $N = 300$. The CVAE (three 256-node hidden layers per encoder/decoder, 10D latent space) is trained using Adam (learning rate 0.001, batch size 256, replay buffer 5000).

Algorithm performance is evaluated via Mean Inverted Generational Distance (MIGD) [11], Mean Hypervolume (MHV) [12], and computational time, measuring convergence/diversity, solution quality, and efficiency, respectively.

B. Results and Discussion

1) MIGD and MHV: As shown in Table II, the proposed framework consistently outperforms the baseline algorithms in terms of both MIGD and MHV metrics across multiple dynamic scenarios.

The superior performance of CVAE-MOEA/D can be attributed to its effective change detection and adaptive response strategies, which enable the algorithm to maintain solution diversity and convergence in the face of dynamic changes. Specifically, CVAE-MOEA/D exhibits a faster convergence rate and lower MIGD values compared to the other algorithms, indicating its effectiveness in tracking the changing POF in dynamic environments. The results demonstrate that the proposed approach can effectively balance economic efficiency and energy self-sufficiency while adapting to time-varying operating conditions.

TABLE II: Performance Comparison of Different Algorithms

Algorithm	MIGD (Mean ± Std)	MHV (Mean ± Std)
DMOEA/D	$0.0449 \pm 5.00\text{E}{-02}$	$0.4473 \pm 9.62\text{E}{-02}$
DNSGA-II(A)	$0.0724 \pm 4.92\text{E}{-02}$	$0.4282 \pm 8.64\text{E}{-02}$
DNSGA-II(B)	$0.0596 \pm 4.52\text{E}{-02}$	$0.4372 \pm 9.66\text{E}{-02}$
PPS-NSGA-II	$0.0563 \pm 3.73\text{E}{-02}$	$0.4433 \pm 9.38\text{E}{-02}$
PPS-MOEA/D	$0.0595 \pm 4.93\text{E}{-02}$	$0.4355 \pm 1.04\text{E}{-01}$
CVAE-MOEA/D	$\mathbf{0.0251 \pm 2.34E{-02}}$	$\mathbf{0.477 \pm 7.60E{-02}}$

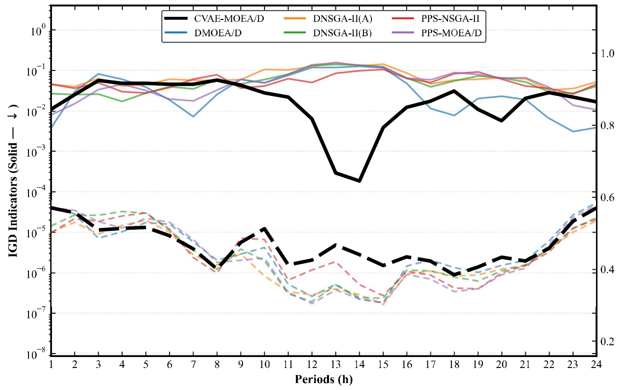

Fig. 3: IGD and HV Convergence

2) IGD and HV Metrics Over Time: We further analyze the convergence behavior of algorithms by plotting the evolution of IGD and HV metrics over time, as illustrated in Fig. 3. From the figure, CVAE-MOEA/D shows competitive performance, with lower IGD values and higher HV values in most time periods along the scheduling horizon. This indicates that CVAE-MOEA/D not only converges faster but also maintains a better spread of solutions over time, effectively capturing the trade-offs between the objectives in a dynamic setting.

3) Dynamic Objective Values Over Time: To visualize the distribution of solutions obtained by different algorithms, we present heatmaps of the objective values across all time periods in Fig. 4.

CVAE-MOEA/D achieves a more uniform and well-distributed POF, effectively capturing the trade-off between the operating cost and external energy supply rate. This indicates that CVAE-MOEA/D can provide decision-makers with a diverse set of high-quality scheduling options under dynamic conditions.

4) Computational Efficiency: As summarized in Table III, CVAE-MOEA/D incurs a higher computational cost compared to DMOEA/D and DNSGA-II variants, while remaining com-

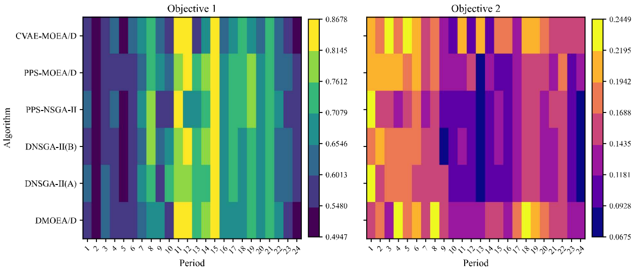

Fig. 4: Objective distributions obtained by different algorithms.

TABLE III: Computational Time Comparison

Algorithm	Computational Time (s)
DMOEA/D	900
DNSGA-II(A)	1020
DNSGA-II(B)	1080
PPS-NSGA-II	1260
PPS-MOEA/D	900
CVAE-MOEA/D	1260

parable to PPS-NSGA-II. This overhead is primarily attributed to the online training of the CVAE and the conditional generation of new populations. Nevertheless, the total execution time remains within a range that is acceptable for practical dynamic optimization in industrial energy systems.

5) Energy Scheduling Results: As depicted in Fig. 5, CVAE-MOEA/D generates feasible 24-period electricity schedules with 100% load satisfaction. It should be noted that the heat and steam demands are also fully met across the entire scheduling horizon, achieving the predefined multi-energy coordination objectives; however, their corresponding profiles are omitted here due to space constraints. By adaptively shifting loads (e.g., reducing peak grid purchases and increasing off-peak charging), the algorithm demonstrates its strong capacity to deliver stable and practical solutions under dynamic environments.

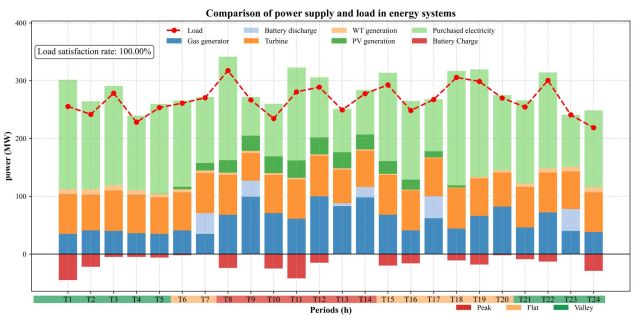

Fig. 5: Electricity supply results obtained by CVAE-MOEA/D.

V. CONCLUSIONS

This paper investigated the dynamic multi-objective scheduling problem of integrated energy systems in steel enterprises under time-varying demands and electricity prices. To address the performance degradation of evolutionary algorithms in such nonstationary environments, a CVAE-assisted dynamic multi-objective optimization framework was proposed. By learning condition-dependent solution distributions from historical high-quality solutions and generating adaptive populations upon environmental changes, the proposed approach enhances the adaptability of evolutionary search in dynamic environments. Experimental results demonstrate improved convergence speed, robustness, and solution stability, as well as reduced operational cost and reliance on external energy sources, validating the effectiveness of the proposed framework for dynamic multi-objective optimization.

ACKNOWLEDGMENT

This research was supported by the Major Program of National Natural Science Foundation of China under Grants 72192830 and 72192831, the 111 Project under Grant B16009, and the Royal Society International Exchanges 2025 Cost Share (NSFC) under Grant IEC\NSFC\252114.

REFERENCES

[1] L. Tang and Y. Meng, "Data analytics and optimization for smart industry," *Frontiers of Engineering Management*, vol. 8, no. 2, pp. 157–171, 2021.
[2] Y. Wang, Z. Liu, C. Cai, L. Xue, Y. Ma, H. Shen, X. Chen, and L. Liu, "Research on the optimization method of integrated energy system operation with multi-subject game," *Energy*, vol. 245, p. 123305, 2022.
[3] Z. Hu, D. He, and H. Zhao, "Multi-objective optimization of energy distribution in steel enterprises considering both exergy efficiency and energy cost," *Energy*, vol. 263, p. 125623, 2023.
[4] J. Ding, C. Yang, Q. Xiao, T. Chai, and Y. Jin, "Dynamic evolutionary multiobjective optimization for raw ore allocation in mineral processing," *IEEE Transactions on Emerging Topics in Computational Intelligence*, vol. 3, no. 1, pp. 36–48, 2019.
[5] J. Han, C. Yang, X. Zhou, and W. Gui, "Dynamic multi-objective optimization arising in iron precipitation of zinc hydrometallurgy," *Hydrometallurgy*, vol. 173, pp. 134–148, 2017.
[6] Q. Zhang and H. Li, "Moea/d: A multiobjective evolutionary algorithm based on decomposition," *IEEE Transactions on evolutionary computation*, vol. 11, no. 6, pp. 712–731, 2007.
[7] Z. Fan, H. Li, C. Wei, W. Li, H. Huang, X. Cai, and Z. Cai, "An improved epsilon constraint handling method embedded in moea/d for constrained multi-objective optimization problems," in *2016 IEEE Symposium Series on Computational Intelligence (SSCI)*, 2016, pp. 1–8.
[8] K. Sohn, H. Lee, and X. Yan, "Learning structured output representation using deep conditional generative models," *Advances in neural information processing systems*, vol. 28, 2015.
[9] K. Deb, U. B. Rao N, and S. Karthik, "Dynamic multi-objective optimization and decision-making using modified nsga-ii: A case study on hydro-thermal power scheduling," in *International conference on evolutionary multi-criterion optimization*. Springer, 2007, pp. 803–817.
[10] A. Zhou, Y. Jin, and Q. Zhang, "A population prediction strategy for evolutionary dynamic multiobjective optimization," *IEEE transactions on cybernetics*, vol. 44, no. 1, pp. 40–53, 2013.
[11] L. Yan, W. Qi, J. Liang, B. Qu, K. Yu, C. Yue, and X. Chai, "Interindividual correlation and dimension-based dual learning for dynamic multiobjective optimization," *IEEE Transactions on Evolutionary Computation*, vol. 27, no. 6, pp. 1780–1793, 2023.
[12] X. Wang, Y. Zhao, L. Tang, and X. Yao, "Moea/d with spatial–temporal topological tensor prediction for evolutionary dynamic multi-objective optimization," *IEEE Transactions on Evolutionary Computation*, vol. 29, no. 3, pp. 764–778, 2025.